Desalination and Water Treatment
www.deswater.com

doi: 10.5004/dwt.2018.22366

114 (2018) 232–241
May

Solid phase extraction of Pb(II) and Cd(II) using reduced graphene oxide-polychloroprene impregnated with magnetic nanoparticle (MNPs-RGO-PCP)

Yousaf Iqbal[a], Rahman Ullah[a], Mansoor Khan[b,*]

[a]*Institute of Chemical Sciences, University of Peshawar, Peshawar, Khyber Pakhtunkhwa, Pakistan, emails: dr.yousaf57@gmail.com (Y. Iqbal), akashchemist@gmail.com (R. Ullah)*
[b]*Department of Chemistry, Kohat University of Science and Technology, Khyber Pakhtunkhwa, Pakistan, email: mansoor009988@gmail.com*

Received 17 December 2017; Accepted 16 April 2018

ABSTRACT

Magnetic solid phase extraction methods for the preconcentration of Pd(II) and Cd(II) was developed by using reduced graphene oxide-polychloroprene impregnated with magnetic nanoparticle (MNPs-RGO-PCP) as an adsorbent. MNPs-RGO-PCP was synthesized and characterized by using Fourier transformation infrared, X-ray diffraction (XRD) and scanning electron microscope. Factors affecting extraction efficiency of the adsorbents such as solution pH, vortex time, adsorbent dose, sample volume and desorption condition were determined and optimized. Analytical parameters such as limit of detection, limit of quantification, linear range, preconcentration factors, enhancement factors and % relative standard deviations were determined under optimized experimental condition. Kinetic study shows that the adsorption of Pb(II) and Cd(II) on MNPs-RGO-PCP follows pseudo-second-order kinetics. The values of thermodynamic parameters such as enthalpy ($\Delta H°$), Gibbs free energy ($\Delta G°$) and entropy ($\Delta S°$) show that the adsorption process is endothermic, spontaneous and feasible in nature. The developed method was applied to certified reference materials such as TMDA 52.2 environmental water, TMDA 62.2 environmental water and SPS-WW2 wastewater with satisfied recovery results. The method was also applied to real environmental samples such as dam water, river water and water from industrial effluent with good addition recovery results.

Keywords: Magnetic solid phase extraction; Polychloroprene; Preconcentration; Impregnated

1. Introduction

Heavy metals are the main cause of water pollution discharge into the water bodies due to many manmade and natural sources [1,2]. These heavy metals cause many harmful effects to the ecosystem [1–4]. Among heavy metals, lead and cadmium are highly toxic and cause severe health problems such as cancer, liver damage, kidney failure, high blood pressure, pulmonary fibrosis, renal edema, skin dermatitis, diarrhea and vomiting [5–12]. Therefore, the accurate and precise determination of these heavy metals in the real water samples is of immense importance. Due to low level of heavy metals in real water samples, their direct determination by using analytical technique is not possible. Therefore, proper preconcentration step prior to its quantification is required [13,14].

Numerous preconcentration methods such as coprecipitation [15], cloud point extraction (CPE) [16], supramolecular solvent-based liquid–liquid extraction [17] and switchable polarity solvent-based liquid phase extraction [18] have been employed for the preconcentration and determination of heavy metals. Certain disadvantages like high amount of toxic organic regent are discharged into the environment and interferences are concerned with these methods [19]. Therefore, solid phase extraction is still a best choice for preconcentration of heavy metals because, its overcame the problems related with other analytical methods [20].

* Corresponding author.

Various solid phase materials such as materials of high surface area like silica gel [21], amberlite [22], activated carbon [23], spent animal bones [24], crab shell; polymeric materials such as ionic imprinted polymer and molecular imprinted polymer [25]; and nanometer size materials such as carbon nanotubes were largely used in the recent past [26,27].

Ye and Shi [28] have synthesized graphene in 2004, having unique properties in various fields. Graphitic carbon possesses sp^2 hybridization with carbon lattice honeycomb in geometry [29]. Due to extremely large surface area and high adsorption capacity, graphene can be used as an excellent solid phase extracting material for trace metals [30]. Due to its high water holding capacity, graphene cannot be separated from the aqueous solution by using ordinary filtration and centrifugation [30]. Therefore, hybrid material of graphene with magnetic nanoparticle was used, so as to separate it by using external magnetic field in order to avoid sample loss during filtration and centrifugation.

In the recent past, large number of polymeric substances is used for the solid phase extraction (SPE) of heavy metals, which include ionic imprinted polymer [31] and molecularly imprinted polymer [32]. Solid phase extraction methods, using polymeric sub- stances as adsorbents, are highly selective in the presence of highly complex matrix nature of the samples.

The aim of the present work is to synthesize magnetic-reduced graphene oxide-polychloroprene (MNPs-RGO-PCP) composite and used as solid phase extracting material for the preconcentration of toxic heavy metals from the environmental water samples.

2. Experimental

2.1. Reagent and standards

All chemicals used were of analytical reagent grade. Polychloroprene (–CH_2CCl=CH–CH_2–) was purchased from Bayer Company, Germany. Standard solutions of Pb(II) and Cd(II) were provided by E. Merck Company (Darmstadt, Germany) using Millipore distilled water. Sodium nitrate ($NaNO_3$), hydrochloric acid (HCl), sulfuric acid (H_2SO_4), ethanol (C_2H_5OH) and toluene (C_7H_8) were provided by Scharlau Company, Spain. Ferric chloride ($FeCl_3$), ferrous sulfate ($FeSO_4$), potassium permanganate ($KMNO_4$), hydrogen peroxide (H_2O_2) and methanol (CH_3OH) were provided by Merck, Darmstadt, Germany, while ammonium hydroxide (NH_4OH) was purchase from Fisher-Scientific Company, UK. Buffer solution of different pH was prepared by using different combination of acids and their salts.

2.2. Instrumentation

Flame atomic absorption spectrometer of model AA 700 (PerkinElmer, USA) was used for absorption measurement of all samples. Mechanical stirrer model (JJ-1 Price time mixer, China) was used for mixing magnetic polymeric composite. Ultrasonic cleaner model (wt-230HTD, Korea) was used for dispersion of reduced graphene oxide (RGO) in the given solvent (toluene). Glass electrode of model 422 WTW, Weilheim, was used for adjustment of pH of all the solution. For Fourier transformation infrared (FTIR) spectra IR Prestigue-21 SHIMADZU HK was used in the range of 4,000–500 cm^{-1}. For surface morphology, scanning electron microscope (SEM) micrographs were taken using 30 kV SEM (JSM5910, JEOL, Japan).

2.3. Preparation of adsorbent

In the present work, adsorbent was prepared in Pakistan Council of Scientific and Industrial Research (PCSIR) laboratories complex, Peshawar, KPK, Pakistan.

2.3.1. Synthesis of graphene oxide

Sodium nitrate (1.0 g) was mixed with sulfuric acid (92.0 mL) at 5°C for 10 min with vigorous stirring and 2.0 g of graphite powder was added to the reaction mixture. After 10 min, 12.0 g of $KMnO_4$ was slowly added to the reaction mixture and allow the reaction for 30 min. The reaction mixture was removed from ice bath and stirred for 30 min at room temperature. Deionized water (184 mL) was added in a dropwise manner with vigorous stirring at 95°C in a reflux condition for 20 min. After that, the reaction mixture was cooled to room temperature and 10 mL of hydrogen peroxide (H_2O_2) was added. The brown-yellow color product was washed with deionized water and 10% HCl to remove unwanted material. The final product was dried in oven at 60°C for 72 h.

2.3.2. Synthesis of reduced graphene oxide

For the synthesis of RGO, 1.0 g of graphene oxide (GO) was ultrasonically dispersed in 200 mL of deionized water for 2 h. Hydrazine hydrate (5.0 mL) was added to the reaction mixture and stirred for an hour at 80°C under the nitrogen atmosphere. The obtained product was filtered, washed with water and ethanol to remove the impurities.

2.3.3. Synthesis of RGO-PCP

Toluene (50 mL) was mixed with 1.0 g of PCP. The mixture was stirred for 2 h under nitrogen atmosphere at 60°C to obtained clear solution. Reduced graphene (0.1 g) was added to the clear solution and dispersed ultrasonically for 2 h. Ethanol (15.0 mL) was added to the reaction mixture to remove unreacted toluene. The resultant composite was then washed with deionized water and dried in a vacuum at 30°C.

2.3.4. Synthesis of magnetic-reduced graphene oxide-polychloroprene (MNPs-RGO-PCP)

Coprecipitation method was used to obtain MNPs-RGO-PCP [33]. For this purpose, salts $FeSO_4.5H_2O$ (1.0 g) and $FeCl_3.6H_2O$ (2.0 mg) were mixed in 70.0 mL of distilled water at 80°C. Ammonia solution (20.0 mL, 20%) was added to the reaction mixture and black precipitates of magnetic nanoparticles (Fe_3O_4) were obtained. To this, 100 mg of RGO-PCP was added at 80°C and allow the reaction for the whole night. The final product obtained was washed several time with distilled water and dried at room temperature.

2.4. Applications of proposed magnetic solid phase extraction

The developed method was applied to certified reference materials (CRMs) such as TMDA 64.2 environmental water,

TMDA 62.2 environmental water and SPS-WW2 wastewater. The method was also applied to real environmental water samples such as river water, pond water and water from industrial effluent. The solid suspended particle from the real water samples were removed and then subjected to the proposed solid phase extraction method, while the CRM water samples were directly used without further purification.

2.5. Magnetic solid phase extraction procedure

Sample solution (10.0 mL) having 15.0 μg of Pb(II) and 25.0 μg Cd(II) was prepared in 50.0 mL centrifuge tube. Desired pH (6.5) was obtained by adding 2 mL of phosphate buffer solution. The sample solution was transferred to another tube having 0.1 g of MNPs-RGO-PCP. The solution was allowed for 3 min under the influence of vortex to ensure complete adsorp- tion of the analyte ions on the adsorbent. The solid phase (MNPs-RGO-PCP) was separated by using external magnetic field and decanted the waste. To the solid phase, 2.0 mL of 0.1 mol L–1 HCl solution was added for desorption of the analyte from the surface of the adsorbent. The concentration of analyte in the eluent solution was determined using atomic absorption spectrometry.

Adsorption capacity (q) was calculated by using the following equation:

$$q = (C_i - C_f)\, m/v \quad (1)$$

where C_i is the initial concentration of analyte, C_f is the final concentration, m is the amount adsorbent and v is the volume of sample.

3. Results and discussion

3.1. Characterization

SEM micrographs of PCP, RGO and reduced graphene oxide-polychloroprene impregnated with magnetic nanoparticle (MNPs-RGO-PCP) were shown in Fig. 1. SEM image of PCP (Fig. 1(a)) shows rough and porous surface morphology. The SEM image of RGO (Fig. 1(b)) shows layered structure of graphene that confirm the successful reduction of GO to RGO. The surface morphology MNPs-RGO-PCP (Fig. 1(c)) shows that the surface of RGO-PCP is successfully impregnate with magnetic nanoparticles.

The FTIR spectra of RGO, PCP and MNPs-RGO-PCP are shown in Fig. 2. The FTIR spectrum of RGO (Fig. 2(a)) at 1,650 can be assigned to C=C stretching vibration. The FTIR spectrum of PCP (Fig. 2(b)) shows sharp peak at 2,919 and 2,844 cm^{-1} can be assigned to C–H stretching vibration and the peak at 1,650 and 821 cm^{-1} can be assigned to C=C and C–Cl, respectively. The FTIR spectrum of MNPs-RGO-PCP shows characteristic peaks at 1,006 and 537 cm^{-1} of MNPs (Fe_3O_4), which confirm the successful impregnation of MNPs on the composite.

X-ray diffraction (XRD) pattern of RGO, PCP and MNPs-RGO-PCP is shown in Fig. 3. XRD pattern (Fig. 3(a)) shows weak and broad peak at 26° that corresponds to reduced graphene. XRD pattern of PCP (Fig. 3(b)) shows amorphous nature of PCP. XRD pat- tern (Fig. 3(c)) of MNPs-RGO-PCP gives characteristic peak at 40° which indicates the face centered cubic crystal of Fe3O4 (JCPDS file card number 19-0629).

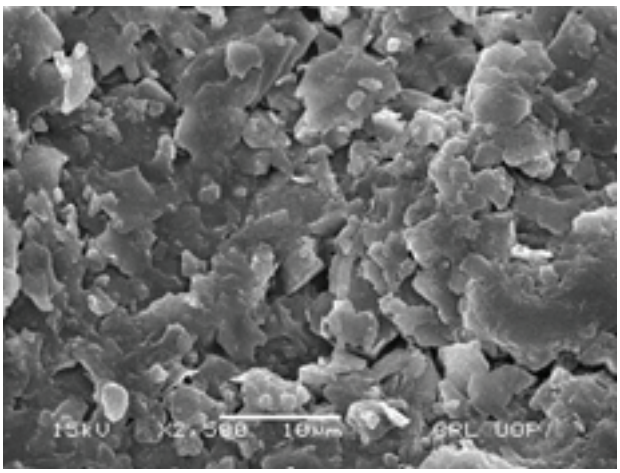

(a)

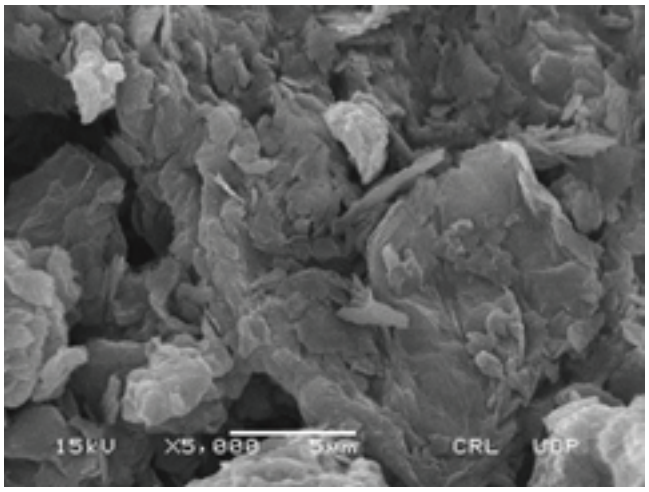

(b)

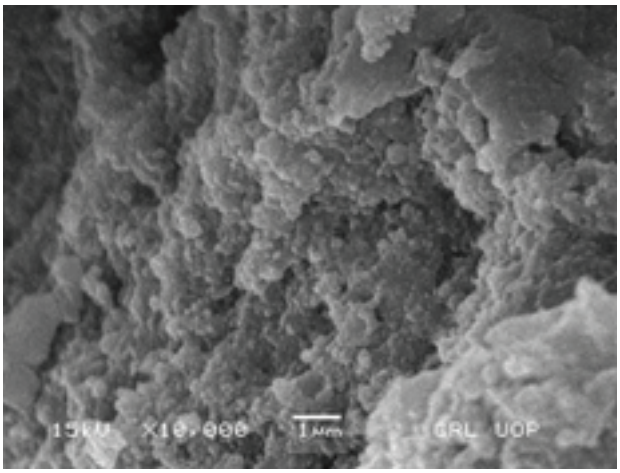

(c)

Fig. 1. SEM images of (a) RGO, (b) PCP and (c) MNPs-RGO-PCP.

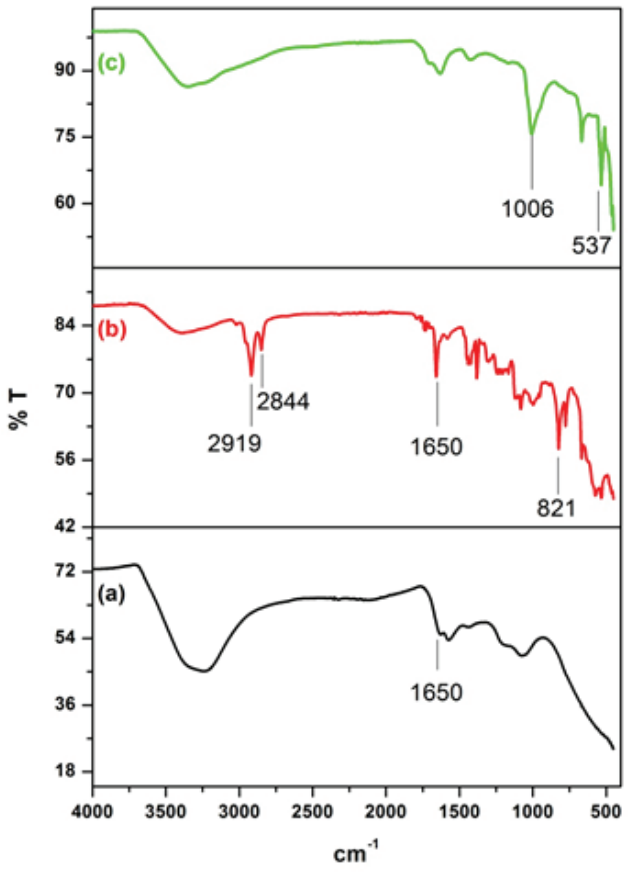

Fig. 2. FTIR spectra of (a) RGO, (b) PCP and (c) MNPs-RGO-PCP.

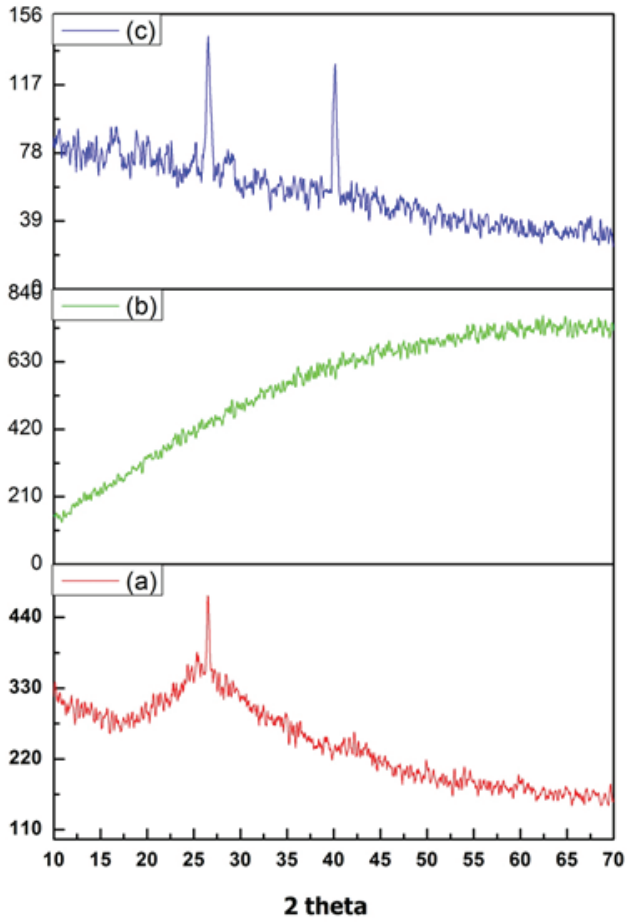

Fig. 3. XRD patterns of (a) RGO, (b) PCP and (c) MNPs-RGO-PCP.

3.2. Effect of pH

pH of the solution is an important parameter that highly affects the efficiency of the adsorbent. For this purpose, preconcentration studies were conducted at different pH ranging from 2 to 9 to obtain the optimum pH as shown in Fig. 4. It can be concluded from Fig. 4 that with increase in pH, the % recovery of Pb(II) and Cd(II) also increases until maximum % recoveries Pb(II) (93 ± 1) and Cd(II) (102 ± 4) were obtained at pH 6.5. Above pH 8, decrease in % recovery of Pb(II) and Cd(II) takes place. Decrease in % recovery at lower pH is due to the positively charged surface of the adsorbent; whereas, at higher pH, metal hydroxide precipitate formation takes place that decreases the % recovery of the analyte ions.

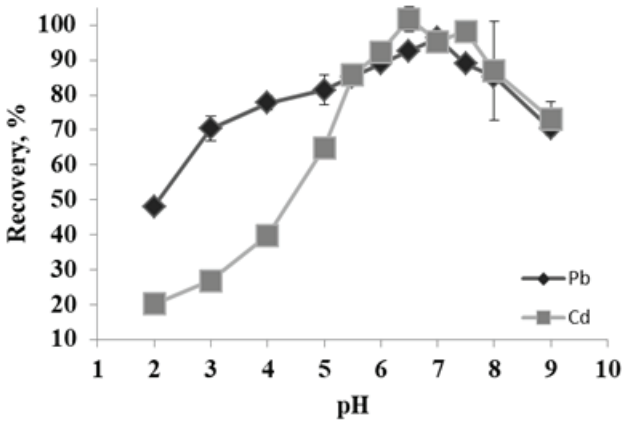

Fig. 4. Effect of pH on % recovery of Pb(II) and Cd(II) using MNPs-RGO-PCP.

3.3. Effect of time

In order to obtain equilibrium time, the % recovery of Pb(II) and Cd(II) was determined at different vortex time ranging from 1 to 10 min as shown in Fig. 5. It can be concluded from Fig. 5 that % recoveries of Pb(II) and Cd(II) increases as the time increases and equilibrium was established in 5 min with quantitative % recoveries of Pb(II) 101 ± 6 and Cd(II) 97 ± 2. Therefore, 5 min of vortex time was used in further preconcentration studies.

3.4. Amount of adsorbent

Different adsorbent doses were used ranging from 20.0 to 150.0 mg to calculate maximum adsorption capacity of the adsorbent at constant adsorbate concentration as shown in Fig. 6. From Fig. 6, it can be concluded that the % recoveries

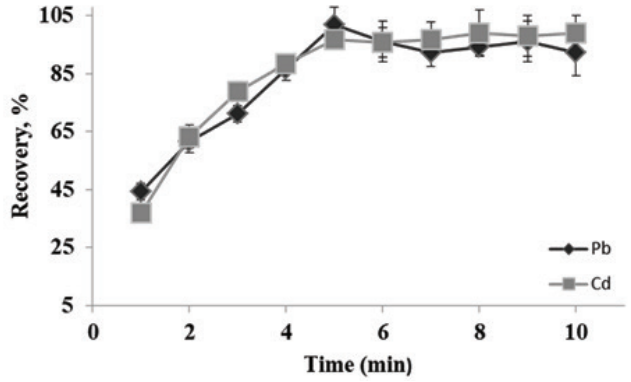

Fig. 5. Effect of vortex time on % recovery of Pb(II) and Cd(II) using MNPs-RGO-PCP.

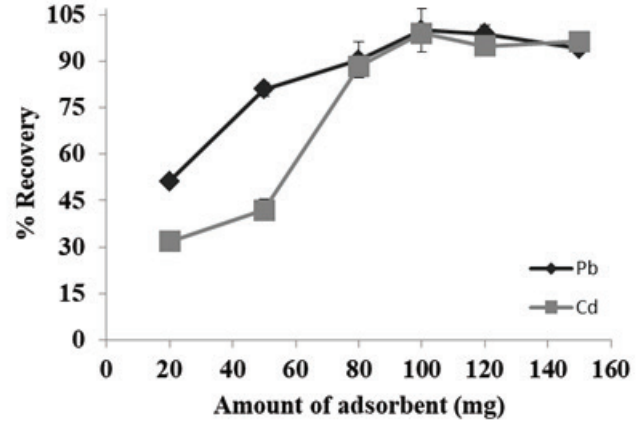

Fig. 6. Effect of adsorbent dose on % recovery of Pb(II) and Cd(II) using MNPs-RGO-PCP.

increase as the amount of adsorbent increases to 100.0 mg (Pb(II) = 100 ± 3 and Cd(II) = 99 ± 1). Further increase in the amount of adsorbent has no effect on % recoveries of analyte ion on MNPs-RGO-PCP.

3.5. Effect of sample volume

The efficiency of the method can be investigated by determining the % recovery at highest sample volume. Therefore, the proposed method was applied to various sample volume ranging from 5 to 50 mL as shown in Fig. 7. It can be seen from Fig. 7 that quantitative % recovery can be obtained up to 30 mL of sample volume. Therefore, preconcentration factor (PF) 15 can be achieved at 30 mL of sample volume and 2 mL of eluent volume.

3.6. Desorption studies

Elution of Pb(II) and Cd(II) from the surface of MNPs-RGO-PCP was carried out using 0.1–0.3 M of HCl and HNO_3 solutions (Table 1). Result shows that 0.2 M HCl is the best choice for elution of analyte metals from the surface of the adsorbent.

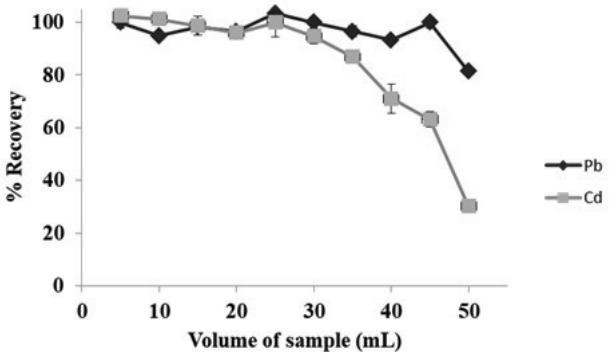

Fig. 7. Effect of sample volume on % recovery of Pb(II) and Cd(II) using MNPs-RGO-PCP.

Table 1
Effect of type and concentration of eluent on percentage recovery of Pb(II) and Cd(II) using MNPs-RGO-PCP (N = 3)

Type and concentration of eluent	% Recovery	
	Pb(II)	Cd(II)
0.1 M HCl	78 ± 2	75 ± 2
0.2 M HCl	96 ± 2	96 ± 3
0.3 M HCl	95 ± 1	93 ± 1
0.1 M HNO_3	73 ± 1	88 ± 3
0.2 M HNO_3	85 ± 3	89 ± 4
0.3 M HNO_3	85 ± 5	90 ± 1

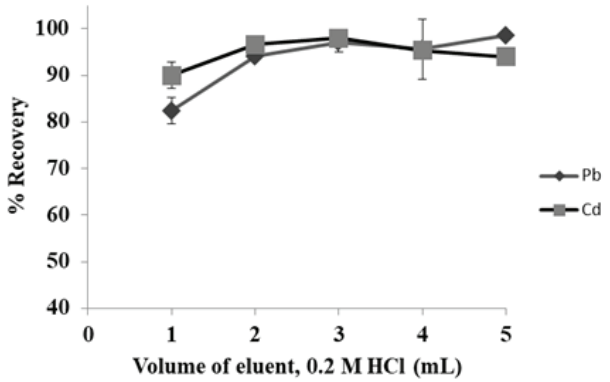

Fig. 8. Effect of eluent volume on % recovery of Pb(II) and Cd(II) using MNPs-RGO-PCP.

For volume optimization, elution was carried out at different volume of 0.2 M HCl ranging from 1 to 5 mL as shown in Fig. 8. The study shows that 2 mL of 0.2 M was enough to obtain maximum elution.

3.7. Matrix effect

In order to examine the selectivity of the method, the proposed SPE method was applied for the preconcentration of Pb(II) and Cd(II) in the presence of different interfering ions which are coexisting with analyte ions in the complex matrix of the environmental samples. Recovery results are shown in Table 2 and shows that the presence of these interfering ions has no significant effect on percentage recovery of the analyte ions. This study ensures that the method is highly selective and free from interferences.

3.8. Kinetic studies

Pseudo-first-order and pseudo-second-order kinetics models were employed in order to explain the mechanism of the adsorption process. For the pseudo-first-order kinetics the following equation was used [34]:

$$\log(q_e - q_t) = \log q_e - \frac{k_1}{2.303}t \quad (2)$$

The values of pseudo-first-order kinetics constant (k_1) and adsorption capacity at equilibrium (q_e) were calculated from slop and intercept as shown in Table 3. Smaller calculated values of adsorption capacities than the experimental adsorption capacities confirmed that pseudo-first-order kinetics is not applicable for the adsorption process.

The pseudo-second-order kinetics model can be expressed as follows [35]:

$$\frac{t}{q_t} = \frac{t}{q_e} + \frac{1}{k_2 q_e^2} \quad (3)$$

The values of pseudo-second-order kinetics constant (k_2) and equilibrium adsorption constant (q_e) were calculated from slop and intercept, respectively, are shown in Table 3. Higher value of correlation coefficient and close agreement between calculated adsorption capacity Pd(II) 0.238 mg g^{-1} and Cd(II) 0.217 mg g^{-1} and experimental adsorption capacity Pd(II) 0.204 mg g^{-1} and Cd(II) 0.198 mg g^{-1} confirmed that the adsorption process follows pseudo-second-order kinetics.

Table 2
Effect of coexisting ions on % recoveries of Pb(II) and Cd(II) using MNPs-RGO-PCP, pH: 6.5, amount of MNPs-RGO-PCP: 0.1 g, volume of sample solution: 10 mL (N = 3)

Interfering ions	Added as	Tolerance level (μg mL^{-1})	% Recovery	
			Pb(II)	Cd(II)
Na^+	NaCl	2,500	93 ± 2	92 ± 4
K^+	KCl	2,500	94 ± 1	96 ± 6
Ca^{2+}	$Ca(NO_3)_2.4H_2O$	500	95 ± 4	98 ± 1
Mg^{2+}	$Mg(NO_3)_2.6H_2O$	500	95 ± 4	96 ± 3
Al^{3+}	$Al(NO_3)_3.7H_2O$	50	94 ± 3	96 ± 4
Cd^{2+}	$Cd(NO_3)_2.6H_2O$	100	99 ± 1	92 ± 1
Zn^{2+}	$Zn(NO_3)_2.6H_2O$	100	91 ± 1	95 ± 4
Fe^{2+}	$Fe(NO_3)_2.6H_2O$	100	93 ± 4	96 ± 4
Cu^{2+}	$Cu(NO_3)_2.6H_2O$	10	93 ± 2	96 ± 1
Ni^{2+}	$Ni(NO_3)_2.6H_2O$	10	97 ± 9	97 ± 1
Mn^{2+}	$Mn(NO_3)_2.6H_2O$	10	97 ± 4	93 ± 1
SO_4^{2-}	Na_2SO_4	1,000	93 ± 3	97 ± 4
CO_3^{2-}	Na_2CO_3	1,000	94 ± 0	95 ± 4
F^-	NaF	100	97 ± 1	94 ± 1

Table 3
Kinetic parameter of the adsorption of Pb(II) and Cd(II) on the surface of MNPs-RGO-PCP

Metal ion	Experimental	Kinetic models					
		Pseudo-first-order			Pseudo-second-order		
	q_e (mg^{-1})	k_1 (min^{-1})	q_e (mg g^{-1})	R^2	k_2 (min^{-1})	q_e (mg g^{-1})	R^2
Cd(II)	0.198	0.523	0.189	0.987	2.557	0.238	0.984
Pb(II)	0.204	0.236	0.107	0.776	3.792	0.217	0.980

Table 4
Thermodynamic parameter for the adsorption of Pb(II) and Cd(II) MNPs-RGO-PCP

Temperature (*K*)	Pb(II)			Cd(II)		
	$\Delta G°$ (kJ mol^{-1})	$\Delta H°$ (kJ mol^{-1})	$\Delta S°$ (kJ mol^{-1})	$\Delta G°$ (kJ mol^{-1})	$\Delta H°$ (kJ mol^{-1})	$\Delta S°$ (kJ mol^{-1})
293	–12.6327	38.876	0.213	–13.490778	22.212	0.108
303	–13.4051			–14.171161		
313	–16.9361			–15.663914		
323	–17.86			–16.41368		
333	–19.1014			–17.803106		
343	–19.947			–18.817799		
353	–21.9513			–22.127804		
363	–23.6369			–24.232684		
373	–27.2025			–26.271316		

3.9. Thermodynamic studies

The spontaneity and feasibility of the adsorption process were investigated by carried out the method at different temperature ranging from 273 to 373 K. For the determination of enthalpy ($\Delta H°$), Gibbs free energy ($\Delta G°$) and entropy ($\Delta S°$) the following equations were used [36,37]:

$$\Delta G° = -RT \ln K_D \quad (4)$$

$$\Delta H° = R\frac{T_2T_1}{T_2 - T_1}\ln\frac{k_2}{k_1} \quad (5)$$

$$\Delta S° = \frac{\Delta H° - \Delta G°}{T} \quad (6)$$

The positive values of $\Delta S°$ and $\Delta H°$ in Table 4 indicate that the adsorption process is endothermic. The decrease in $\Delta G°$ values with increase in temperature confirms that metal uptake increase with increase in temperature.

3.10. Analytical performance

Analytical parameters such as limit of detection (LOD), limit of quantification (LOQ), PF, enhancement factor (EF) and percentage relative standard deviation (% RSD) were determined under optimized experimental condition (Table 5). LOD and LOQ were calculated from 3 to 10 time of the ratio of the standard deviation of 10 blank absorbance's to the slop of regression equation, respectively. PF was calculated from the ratio of the highest sample volume to the final volume. EF was calculated from the ratio of slopes of regression equations before and after preconcentration. RSD was determined from five repeated determination of known concentration of sample.

3.11. Validation of the method

Validation of the proposed magnetic solid phase extraction method was carried out by applying the method to CRM (TMDA 52.2 environmental water, TMDA 62.2 environmental water and SPS-WW2 wastewater) and the % recovery results are shown in Table 6. The quantitative % recovery shows that the method can be successfully applied to trace metal analysis.

Table 5
Analytical parameters of the develop method

Analytical parameter	Pb(II)	Cd(II)
Limit of detection (μg L^{-1})	1.22	0.21
Limit of quantification (μg L^{-1})	4.09	0.69
Preconcentration factor (PF)	15	15
Linear range (μg mL^{-1})	0.2–2.4	0.2–2.4
Enhancement factor (EF)	15	15
Relative standard deviation (%)	5.1	4.5
Correlation coefficient (R^2)	0.995	0.972

The method was also applied to real environmental water sample for addition recovery. For this purpose, water samples from river, dam and industrial area were collected and subjected to the developed method. The % recovery results are shown in Table 7 and also show that the method can be successfully applied to real environmental sample with satisfactory recovery results.

The proposed solid phase extraction was compared with other extraction methods in the literature regarding the values of LOD, PF and EF (Table 8). It can be concluded that the developed method is either superior or similar in extraction efficiency of other extraction studies given in the literature.

4. Conclusion

- Development of solid phase extraction method for the preconcentration of Pb(II) and Cd(II) using MNPs-RG-PCP as an adsorbent.
- The adsorbent was novel and efficient for the adsorption Pb(II) and Cd(II).
- The method is highly sensitive with low LOD value, reproducible with low value % RSD and efficient with high values of PF and EF.

Table 6
Validation of the proposed solid phase extraction of Pb and Cd using CRM

Certified reference material	Pb(II)			Cd(II)		
	Certified value (μg mL^{-1})	Found value (μg mL^{-1})	Recovery %	Certified value (μg mL^{-1})	Found value (μg mL^{-1})	Recovery %
SPS-WW2	0.500	0.498 ± 0.009[a]	100[b]	0.300	0.290 ± 0.006	97
TMDA 64.4	0.286	0.280 ± 0.005	98	0.253	0.250 ± 0.012	99
TMDA 62.2	0.0984	0.0952 ± 5.0	97	95.0	0.092 ± 0.003	97

[a]Mean of three determinations ± standard deviation.
[b]% Recovery = (observed value/expected value) × 100.

Table 7
Addition recovery results for Pb(II) and Cd(II) using the proposed solid phase extraction method, pH: 6.5, amount of MNPs-RGO-PCP: 0.1 g, volume of sample: 15 mL, final volume: 2 mL (N = 3)

Sample	Pb(II)			Cd(II)		
	Added (μg mL^{-1})	Found (μg mL^{-1})	Recovery %	Added (μg mL^{-1})	Found (μg mL^{-1})	Recovery %
River water	0.0	BDL	–	0.0	0.100 ± 0.008	–
	0.6	0.562 ± 0.008	94	0.6	0.700 ± 0.001	100
	1.0	0.981 ± 0.002	98	1.0	0.993 ± 0.001	99
Pond water	0.0	BDL	–	0.0	0.450 ± 0.020	–
	0.5	0.493 ± 0.007	99	0.5	0.920 ± 0.010	94
	0.8	0.772 ± 0.001	96	0.8	1.260 ± 0.005	101
Industrial water	0.0	BDL	–	0.0	BDL	–
	0.3	0.306 ± 0.002	102	0.3	0.280 ± 0.003	93
	0.5	0.725 ± 0.004	104	0.5	0.460 ± 0.002	92

Table 8
Comparison of the proposed solid phase extraction method with other extraction methods in the literature

Method	Analysis	Detection limit (μg L^{-1})	Sample	References
SPE[a]	FAAS	Cd(II): 0.6, Pb(II): 6.6	Water, food	[38]
SPE	FAAS	Pb(II): 3.9, Co(II): 2.9	Environment	[39]
CPE		Pd(II): 2.6, Cd: 1.4	Water and Food	[40]
IL-DLLME[c]	PZAAS[g]	Pb(II): 9.5	Environment	[41]
DLLME	GFAAS[h]	Co(II): 0.03	Rice and water	[42]
SPE	FAAS	Pb(II): 1.22, Cd(II): 0.21	Water	This work

- The method is environment-friendly as no toxic chemicals are discharged to the environment.
- The method can be successfully applied to natural water sample irrespective to their complex matrix nature.

References

[1] M. Khan, E. Yilmaz, M. Soylak, Vortex assisted magnetic solid phase extraction of lead (II) and cobalt (II) on silica coated magnetic multiwalled carbon nanotubes impregnated with 1-(2-pyridylazo)-2-naphthol, J. Mol. Liq., 224 (2016) 639–647.
[2] S.Z. Mohammadi, A. Seyedi, Preconcentration of cadmium and copper ions on magnetic core–shell nanoparticles for determination by flame atomic absorption, Toxicol. Environ. Chem., 98 (2016) 705–713.
[3] J. Shah, M.R. Jan, M. Khan, S. Amir, Removal and recovery of cadmium from aqueous solutions using magnetic nanoparticle-modified sawdust: kinetics and adsorption isotherm studies, Desal. Wat. Treat., 57 (2016) 9736–9744.
[4] M. Khan, J. Shah, M.R. Jan, Magnetic solid phase extraction of Cd (II) using magnetic nanoparticle (MNPs) and silica coated magnetic nanoparticles (SiMNPs) from environmental water samples, Desal. Wat. Treat., 83 (2017) 123–132.

[5] E. Yilmaz, M. Soylak, Ionic liquid-linked dual magnetic microextraction of lead (II) from environmental samples prior to its micro-sampling flame atomic absorption spectrometric determination, Talanta, 116 (2013) 882–886.
[6] S.K. Wadhwa, M. Tuzen, T.G. Kazi, M. Soylak, B. Hazer, Polyhydroxybutyrate-b-polyethyleneglycol block copolymer for the solid phase extraction of lead and copper in water, baby foods, tea and coffee samples, Food Chem., 152 (2014) 75–80.
[7] J. Duruibe, M. Ogwuegbu, J. Egwurugwu, Heavy metal pollution and human biotoxic effects, Int. J. Phys. Sci., 2 (2007) 112–118.
[8] M. Behbahani, P.G. Hassanlou, M.M. Amini, F. Omidi, A. Esrafili, M. Farzadkia, A. Bagheri, Application of solvent-assisted dispersive solid phase extraction as a new, fast, simple and reliable preconcentration and trace detection of lead and cadmium ions in fruit and water samples, Food Chem., 187 (2015) 82–88.
[9] M.H. Mashhadizadeh, Z. Karami, Solid phase extraction of trace amounts of Ag, Cd, Cu, and Zn in environmental samples using magnetic nanoparticles coated by 3-(trimethoxysilyl)-1-propantiol and modified with 2-amino-5-mercapto-1,3,4-thiadiazole and their determination by ICP-OES, J. Hazard. Mater., 190 (2011) 1023–1029.
[10] S. Khan, T.G. Kazi, M. Soylak, Rapid ionic liquid-based ultrasound assisted dual magnetic microextraction to preconcentrate and separate cadmium-4-(2-thiazolylazo)-resorcinol complex from environmental and biological samples, Spectrochim. Acta, Part A, 123 (2014) 194–199.
[11] N. Jalbani, E. Yilmaz, R. Alosmanov, M. Soylak, Solid-phase extraction of copper and zinc in water samples using diethylamine-modified phosphorus-containing polymer, Desal. Wat. Treat., 57 (2016) 2834–2842.
[12] S. Khan, E. Yilmaz, T.G Kazi, M. Soylak, Vortex assisted liquid–liquid microextraction using triton X-114 for ultratrace cadmium prior to analysis, Clean–Soil, Air, Water, 42 (2014) 1083–1088.
[13] M.H. Mashhadizadeh, M. Amoli-Diva, M. Shapouri, H. Afruzi, Solid phase extraction of trace amounts of silver, cadmium, copper, mercury, and lead in various food samples based on ethylene glycol bis-mercaptoacetate modified 3-(trimethoxysilyl)-1-propanethiol coated Fe_3O_4 nanoparticles, Food Chem., 151 (2014) 300–305.
[14] M. Wierucka, M. Biziuk, Application of magnetic nanoparticles for magnetic solid-phase extraction in preparing biological, environmental and food samples, TrAC, Trends Anal. Chem., 59 (2014) 50–58.
[15] T. Oymak, S. Tokalıoğlu, V. Yılmaz, Ş. Kartal, D. Aydın, Determination of lead and cadmium in food samples by the coprecipitation method, Food Chem., 113 (2009) 1314–1317.
[16] N. Jalbani, M. Soylak, Preconcentration/separation of lead at trace level from water samples by mixed micelle cloud point extraction, J. Ind. Eng. Chem., 29 (2015) 48–51.
[17] M. Khan, M. Soylak, Supramolecular solvent based liquid–liquid microextraction of aluminum from water and hair samples prior to UV-visible spectrophotometric detection, RSC Adv., 5 (2015) 62433–62438.
[18] M. Khan, M. Soylak, Switchable solvent based liquid phase microextraction of mercury from environmental samples: a green aspect, RSC Adv., 30 (2016) 24968–24975.
[19] M. Khan, E. Yilmaz, B. Sevinc, E. Sahmetlioglu, J. Shah, M.R. Jan, M. Soylak, Preparation and characterization of magnetic allylamine modified graphene oxide-poly (vinyl acetate-co-divinylbenzene) nanocomposite for vortex assisted magnetic solid phase extraction of some metal ions, Talanta, 146 (2016) 130–137.
[20] Z.A. ALOthman, E. Yilmaz, M.A. Habila, I.H. Alsohaimi, A.M. Aldawsari, N.M. AL-Harbi, M. Soylak, Triethylenetetramine modified multiwalled carbon nanotubes for the efficient preconcentration of Pb (II), Cu (II), Ni (II) and Cd (II) before FAAS detection, RSC Adv., 5 (2015) 106905–106911.
[21] G. Zhou, C. Liu, Y. Tang, S. Luo, Z. Zeng, Y. Liu, R. Xu, L. Chu, Sponge-like polysiloxane-graphene oxide gel as a highly efficient and renewable adsorbent for lead and cadmium metals removal from wastewater, Chem. Eng. J., 280 (2015) 275–282.
[22] M. Naushad, Z.A. ALOthman, G. Sharma, Kinetics, isotherm and thermodynamic investigations for the adsorption of Co (II) ion onto crystal violet modified amberlite IR-120 resin, Ionics, 21 (2015) 1453–1459.
[23] T. Bohli, A. Ouederni, N. Fiol, I. Villaescusa, Evaluation of an activated carbon from olive stones used as an adsorbent for heavy metal removal from aqueous phases, C.R. Chim., 18 (2015) 88–99.
[24] M.J. Amiri, J. Abedi-Koupai, S.S. Eslamian, M. Arshadi, Adsorption of Pb (II) and Hg (II) ions from aqueous single metal solutions by using surfactant-modified ostrich bone waste, Desal. Wat. Treat., 57 (2016) 16522–16539.
[25] M. Behbahani, P.G. Hassanlou, M.M. Amini, H.R. Moazami, H.S. Abandansari, A. Bagheri, S.H. Zadeh, Selective solid-phase extraction and trace monitoring of lead ions in food and water samples using new lead-imprinted polymer nanoparticles, Food Anal. Methods, 8 (2015) 558–568.
[26] M. Yusuf, F. Elfghi, S.A. Zaidi, E. Abdullah, M.A. Khan, Applications of graphene and its derivatives as an adsorbent for heavy metal and dye removal: a systematic and comprehensive overview, RSC Adv., 5 (2015) 50392–50420.
[27] A. Abbas, M.A. Al-Amer, T.M. Laoui, M.J. Al-Marri, M.S. Nasser, M. Khraisheh, M.A. Atieh, Heavy metal removal from aqueous solution by advanced carbon nanotubes, Crit. Rev. Anal. Chem., 157 (2016) 141–161.
[28] N. Ye, P. Shi, Applications of graphene-based materials in solid-phase extraction and solid-phase microextraction, Sep. Purif. Rev., 44 (2015) 183–198.
[29] J.-P Fan, B. Zheng, Y. Qin, D. Yang, D.-D. Liao, X.-K. Xu, X.-H. Zhang, J.-H. Zhu, A superparamagnetic Fe_3O_4-graphene oxide nanocomposite for enrichment of nuciferine in the extract of *Nelumbinis Folium* (Lotus leaf), Appl. Surf. Sci., 364 (2016) 332–339.
[30] J. Sun, Q. Liang, Q. Han, X. Zhang, M. Ding, One-step synthesis of magnetic graphene oxide nanocomposite and its application in magnetic solid phase extraction of heavy metal ions from biological samples, Talanta, 132 (2015) 557–563.
[31] H.R. Rajabi, M. Shamsipur, M.M. Zahedi, M. Roushani, On-line flow injection solid phase extraction using imprinted polymeric nanobeads for the preconcentration and determination of mercury ions, Chem. Eng. J., 259 (2015) 330–337.
[32] D.L. Huang, R.Z. Wang, Y.G. Liu, G.M. Zeng, C. Lai, P. Xu, B.A. Lu, J.J. Xu, C. Wang, C. Huang, Application of molecularly imprinted polymers in wastewater treatment: a review, Environ. Sci. Pollut. Res., 22 (2015) 963–977.
[33] W. Wu, Z. Wu, T. Yu, C. Jiang, W.S. Kim, Recent progress on magnetic iron oxide nanoparticles: synthesis, surface functional strategies and biomedical applications, Sci. Technol. Adv. Mater., 16 (2015) 023501.
[34] M.S. Gasser, G.A. Morad, H.F. Aly, Batch kinetics and thermodynamics of chromium ions removal from waste solutions using synthetic adsorbents, J. Hazard. Mater., 142 (2007) 118–129.
[35] S. Yadav, V. Srivastava, S. Banerjee, C.H. Weng, Y.C. Sharma, Adsorption characteristics of modified sand for the removal of hexavalent chromium ions from aqueous solutions: kinetic, thermodynamic and equilibrium studies, CATENA, 100 (2013) 120–127.
[36] W. Konicki, I. Pełech, E. Mijowska, I. Jasińska, Adsorption of anionic dye Direct Red 23 onto magnetic multi-walled carbon nanotubes-Fe_3C nanocomposite: kinetics, equilibrium and thermodynamics, Chem. Eng. J., 210 (2012) 87–95.
[37] V.K. Gupta, C. Jain, I. Ali, M. Sharma, V. Saini, Removal of cadmium and nickel from wastewater using bagasse fly ash—a sugar industry waste, Water Res., 37 (2003) 4038–4044.
[38] M. Habila, E. Yilmaz, Z.A. Alothman, M. Soylak, Flame atomic absorption spectrometric determination of Cd, Pb, and Cu in food samples after pre-concentration using 4-(2-thiazolylazo) resorcinol-modified activated carbon, J. Ind. Eng. Chem., 20 (2014) 3989–3993.
[39] M. Tuzen, K.O. Saygi, C. Usta, M. Soylak, *Pseudomonas aeruginosa* immobilized multiwalled carbon nanotubes as biosorbent for heavy metal ions, Bioresour. Technol., 99 (2008) 1563–1570.

[40] M. Ghaedi, A. Shokrollahi, K. Niknam, E. Niknam, A. Najibi, M. Soylak, Cloud point extraction and flame atomic absorption spectrometric determination of cadmium(II), lead(II), palladium(II) and silver(I) in environmental samples, J. Hazard. Mater., 168 (2009) 1022–1027.
[41] H. Bai, Q. Zhou, G. Xie, J. Xiao, Temperature-controlled ionic liquid–liquid-phase microextraction for the pre-concentration of lead from environmental samples prior to flame atomic absorption spectrometry, Talanta, 80 (2010) 1638–1642.
[42] H. Jiang, Y. Qin, B. Hu, Dispersive liquid phase microextraction (DLPME) combined with graphite furnace atomic absorption spectrometry (GFAAS) for determination of trace Co and Ni in environmental water and rice samples, Talanta, 74 (2008) 1160–1165.